

Comparison and Combination of Iris Matchers for Reliable Personal Authentication

Ajay Kumar, Arun Passi

Abstract: *The personal identification approaches using iris images are receiving increasing attention in the biometrics literature. Several methods have been presented in the literature and those based on the phase encoding of texture information are suggested to be the most promising. However, there has not been any attempt to combine these approaches to achieve further improvement in the performance. This paper presents a comparative study of the performance from the iris authentication using Log-Gabor, Haar wavelet, DCT and FFT based features. Our experimental results suggest that the performance from the Haar wavelet and Log-Gabor filter based phase encoding is the most promising among all the four approaches considered in this work. Therefore the combination of these two matchers is most promising, both in terms of performance and the computational complexity. Our experimental results from the all 411 users (CASIA v3) and 224 users (IITD v1) database illustrate significant improvement in the performance which is not possible with either of these approaches individually.*

1. Introduction

The iris identification has emerged as a preferred modality for large-scale user authentication and has significantly higher user-acceptance as compared to the more reliable retinal identification. The iris patterns are highly stable and unique as the probability for the existence of two irises that are same has been theoretically

estimated to be very high, *i.e.* one in 10^{72} [8]. Although the performances from the iris patterns have been extensively evaluated in the literature, it is often inadequate to meet the rigorous requirement for very large scale applications. The personal identification approaches using multi-biometrics (multi-algorithm, multi-features, multi-classifiers, *etc.*) are more promising for such applications and are yet to be investigated for performance improvement using iris images.

Related Work and Motivation

The iris identification using analysis of the iris texture has attracted lot of attention and researchers have presented variety of approaches in the literature [1]-[10]. Daugman [2], [22] has presented highly accurate 2D Gabor filter based approach for the iris identification system that employed 2048 bit iris-code. He has also presented [21] the most promising experimental results from large-scale *private* database. Boles [5] has detailed fine-to-coarse approximation at different resolution levels that are based on zero-crossing representation from the wavelet transform decomposition. Wildes *et al.* [7] have focused on efficient implementation of gradient-based iris segmentation using Laplacian pyramid. Proença and Alexandre [8] have suggested region-based feature extraction for the iris images acquired from large distances. Thornton *et al.* [1] have recently estimated the non-linear deformations from the iris patterns and proposed a Bayesian approach for reliable performance improvement.

Huang *et al.* [20] have demonstrated the usage of phase-based local correlations for matching iris patterns and achieved notable performance over the prior techniques. Li Ma *et al.* [4], [6] employed multi-scale bandpass decomposition and evaluated comparative performance from prior approaches. They also presented [24] an effective alternative for iris identification using Gaussian-Hermite moments extracted from 1-D iris intensity signals. The compact representation of iris features using moment invariants extracted from the Gabor wavelet features has shown to offer attractive performance and detailed in [22]. Sanchez-Avila *et al.* [30] have made promising improvement in the method suggested in [5]. Accurate segmentation of iris and eyelash regions is the key for the accurate iris recognition and has been the focus of study in [26] and [27]. Motivated by the success of minutiae representation commonly employed in fingerprint representation, Yu *et al.* [28] have attempted to extract key points from iris texture and illustrated promising results.

The summary of prior work on the iris identification suggests that there has not been any attempt to combine the promising approaches presented in the literature and investigate the performance improvement. It may be noted that such combination should have the merit of improved accuracy and requires relative performance analysis of the candidate approaches. It is generally believed that the acquisition of large number of images for user registration (or for the offline training of biometric

system) causes inconvenience to the users and therefore smaller number of training images is always desirable for the performance evaluation. Therefore the performances from the prior approaches, or from the proposed combination methods, need to be evaluated using minimum[†] training set to ascertain its effectiveness.

2. Our Work

The work detailed in this paper focuses on the comparative performance evaluation of the phase encoding of iris patterns using four approaches; Haar wavelet, Gabor filter, Discrete Cosine Transform (DCT), and Fast Fourier Transform (FFT) based feature extraction. The combination of the best performing approaches is used to investigate the further performance improvement. The experimental results detailed in this paper suggest that the performance from the Haar wavelet and Log-Gabor filter based phase encoding is the most promising among all the four approaches considered in this paper. Therefore simultaneously extracted matching scores from these two matchers are combined to achieve further performance improvement. The prior work in the literature of iris identification approaches illustrated promising performance but with the usage of several training images. Therefore another objective of this work is to evaluate the comparative performance of various approaches with only *one* training image. The performance from the developed system, using the combination of

[†] The minimum or one training image performance is of significant interest in the forensic analysis.

matchers, is extensively evaluated using *one* training image on publicly available CASIA [15] and IITD database [16].

Our implementation of the considered four approaches is largely based on their details presented in the literature. While evaluating these approaches, various combinations of parameters are attempted, separately for three different databases, to achieve the best possible performance. The performance from the developed online system is evaluated on newly acquired IITD iris image database, which is being made available freely for the researchers. The following sections 2.1-2.4 briefly describe these matchers and our implementation for the performance evaluation. The image normalization steps involving the segmentation of iris and eyelash regions are detailed in section 3. The rigorous experimental results from three different iris databases are detailed in section 4 which is followed by the discussion on the results and the contributions of this paper. Finally the section 6 summarizes the main conclusions from this paper.

2.1 Discrete Cosine Transform

The iris recognition using the phase information from the zero crossings of the one dimensional DCT has shown promising results in [3]. The DCT coefficients $C(u)$ from the signal $f(x)$ of length L are obtained as follows:

$$C(u) = \varepsilon(u) \sum_{x=0}^{L-1} f(x) \cos\left[\frac{\pi u}{2L}(2x+1)\right], \quad \forall u = 0, 1, \dots, L-1 \quad (1)$$

where $\varepsilon(u) = \frac{2}{L}$ for $u \neq 0$ and $\varepsilon(u) = \frac{2\sqrt{2}}{L}$ for $u = 0$. Our implementation of this approach was iteratively tuned to achieve the best performance (as illustrated from various results in figure 1). The skewing of successive rows by one pixel to the right was used to extract the blocks orientated at 45° . Then the weighted average under a $1/4^{\text{th}}$ Hanning window is performed on each block which reduces the horizontal resolution and the degrading effects of noise and generates a 1D vector. That vector is then windowed using a similar Hanning window in the vertical direction before the application of DCT. Now, difference of adjacent DCT output vectors are calculated and feature vector is formed from their zero crossings. The size of the feature vector depends on the amount of information (bits) retained after the application of DCT. For matching of two iris templates a modified version of hamming distance is used in which the product of sum of respective bits corresponding to each block:

$$S = \left(\prod_{i=1}^M \frac{\sum_{j=1}^N \text{Block1}_{ij} \oplus \text{Block2}_{ij}}{N} \right)^{1/M} \quad (2)$$

where, M is the number of bits per block in vertical direction, N is the total number of blocks. This method of consolidating the hamming distance can improve the genuine matches by skewing the matching scores S towards zero and also improve the imposter matches by skewing the corresponding scores S towards 0.5 [3]. The figure 1 illustrates the selection of block size and their orientation (skew) from the achieved performance when only one image was used for the training and rest six images are

used for evaluation. The receiver operating characteristics (ROC) in figure 1 shows the variation of genuine acceptance rate (GAR) with corresponding false acceptance rate (FAR). The evaluation results shown in figure 1 suggest that the block size of 8×12 , with overlapping of 4 pixels vertically and 6 pixels horizontally, achieves the best results. Similarly, these results also suggest that higher performance is achieved when the size of Hanning window is chosen to be equal to the width and height of the corresponding block, and the blocks are oriented at 45° (achieved by skewing of successive rows of the image by one pixel).

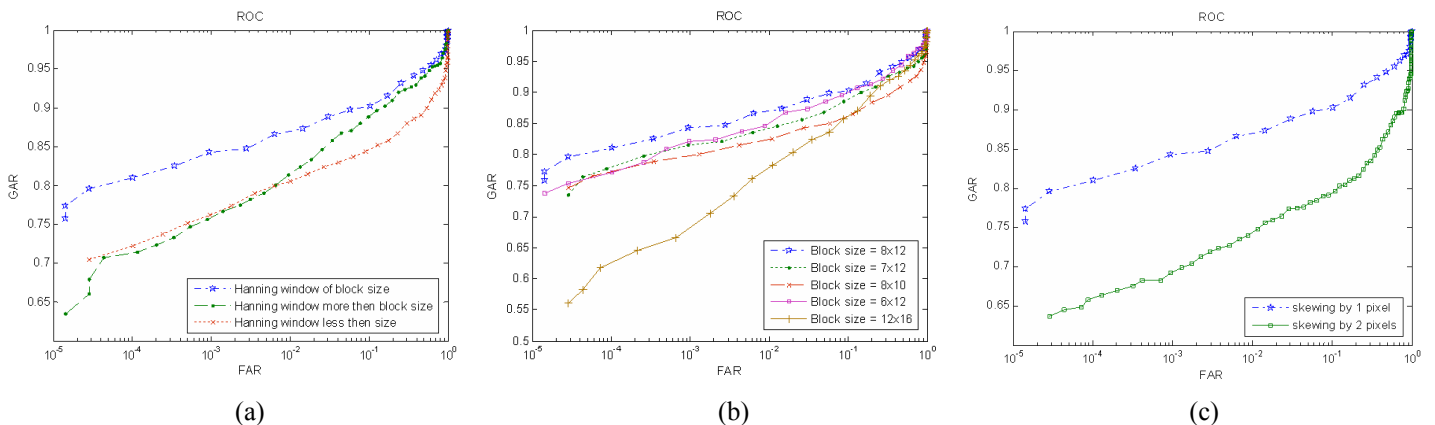


Figure 1: Selection of block size from the resulting performance using one training in (a) and (b), and the corresponding performance from block orientation.

2.2 Fast Fourier Transform

The local frequency variations can also be employed for encoding the phase information from the iris texture. The enhanced iris images are firstly divided into block aligned at 45° . The blocks are then averaged in the horizontal direction and then multiplied by a Hanning window, which results in a 1-D signal corresponding to each

block. This signal $f(x)$ is employed to extract the one dimensional FFT coefficients,

$F(k)$, as follows:

$$F(k) = \sum_{x=1}^L f(x) \exp\left\{\frac{-2\pi j(k-1)x}{L}\right\}, \quad \forall k = 1, 2, \dots, L \quad (3)$$

The difference in the magnitude of adjacent blocks is computed and a binary feature vector is formed from the zero crossings of each difference. The size of the blocks was chosen to be 8×12 with an overlapping of 4 pixels in the vertical direction and 6 pixels in the horizontal direction. The size of the resulting feature vector was 8160 bits and Hamming distance was used to measure the difference between the feature vectors.

2.3 Haar Wavelet

The texture details in the iris region can be analyzed at different resolutions using its multiscale wavelet decomposition. The Haar wavelets can capture sharp discontinuities in the spatial gray-level texture by repeated application of following low-pass (g) and high-pass (h) filters [9]:

$$g = \frac{1}{\sqrt{2}}[1 \ 1], \quad h = \frac{1}{\sqrt{2}}[1 \ -1] \quad (4)$$

The above filters are separately applied to the rows and columns of the iris images resulting in four channel filter bank with channels LL, LH, HL, and HH corresponding to filters $g^t * g$, $g^t * h$, $h^t * g$, and $h^t * h$ respectively. The recursive application of this decomposition is used to construct higher level decomposition. The feature extraction using the four-level Haar wavelet decomposition [10] of the

enhanced image was firstly investigated. The diagonal coefficients of the fourth level were employed to obtain 4×32 real values. In addition to these 128 values, the average of diagonal coefficients from the first, second and third level decomposition were also employed. Each of those 131 ($3 + 128$) values were quantized to binary values by simply converting the positive values to 1 and negative values to 0. Therefore, the feature vector for any iris constituted of only 131 bits. The Hamming distance was again employed to match two feature vectors. However, as shown in figure 2, the performance from these features was poor and therefore we also investigated performance using higher level wavelet coefficients as suggested in [11].

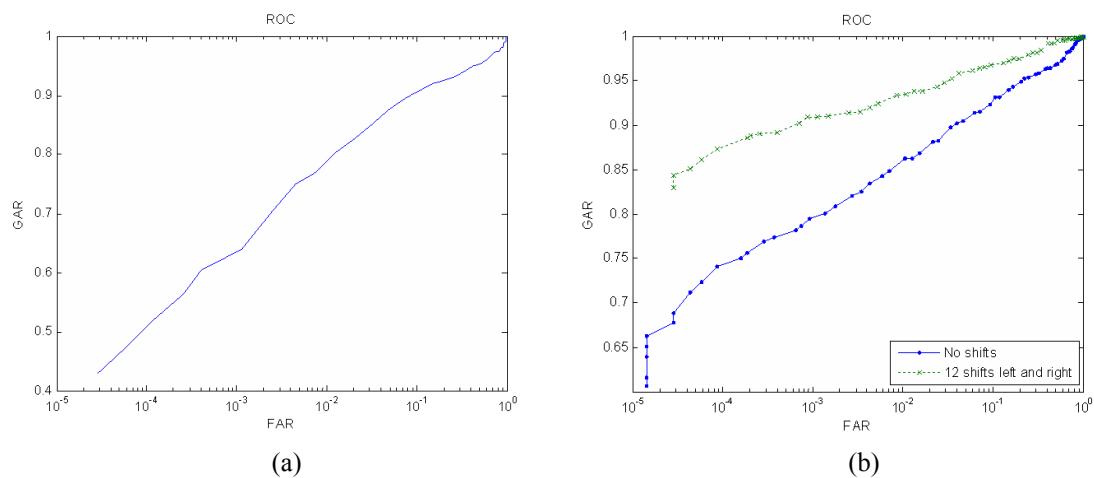


Figure 2: The performance from the Haar wavelet based approach using 4 level decomposition as detailed in [10] and (a) and 5-level decomposition in (b).

In this approach, the enhanced images are decomposed into 5 levels by the Haar wavelets. Next the vertical, horizontal and diagonal coefficients of 4th and 5th level were employed. The coefficients of 1st, 2nd, and 3rd level were almost the same as those of the 4th level and therefore the smallest of them (4th level coefficients) were

employed and rest were ignored. The 5th level decomposition offered the most discriminative information and therefore all the coefficients from this decomposition were employed. The phase encoding from the zero crossings of the coefficients formed the binary values of the feature vector. The size of this feature vector was 3 times the size of features of 4th level (4×32) plus 3 times the features of 5th level (2×16), therefore in total the size of feature vector was 480 bits. The Hamming distance was then employed to ascertain the matching distance between feature vectors. The feature vectors are shifted left and right bit-wise and the lowest from the number of hamming distances calculated from successive shifts is employed. The shifting of feature vectors to the left and right by 12 bits can account for the possible rotation of the extracted iris and significantly improved the performance as shown in figure 2 (one training image and seven test images per user).

2.4 Gabor Filter

The features extracted from the phase encoding of iris texture has gained lot of attention since the fundamental work of Daugman [2]. The response from the bank of 2D Gabor filters can reliably encode the phase information in the iris texture and has shown to offer promising performance. However, the Gabor filters over represent the low frequency components and under represent the high frequency components in any encoding, and an even-symmetric Gabor filter will have a DC component whenever the bandwidth is larger than one octave. Therefore the Log-Gabor filters have been

recently suggested [12]-[13] for phase encoding because the zero DC-component can be obtained for any bandwidth by using a Gabor filter which is Gaussian on a logarithmic scale. The Log-Gabor filters having extended tails at the high frequency end are expected to offer more efficient encoding of natural images [14]. Figure 3 shows real and imaginary components of a typical 1-D Log-Gabor filter.

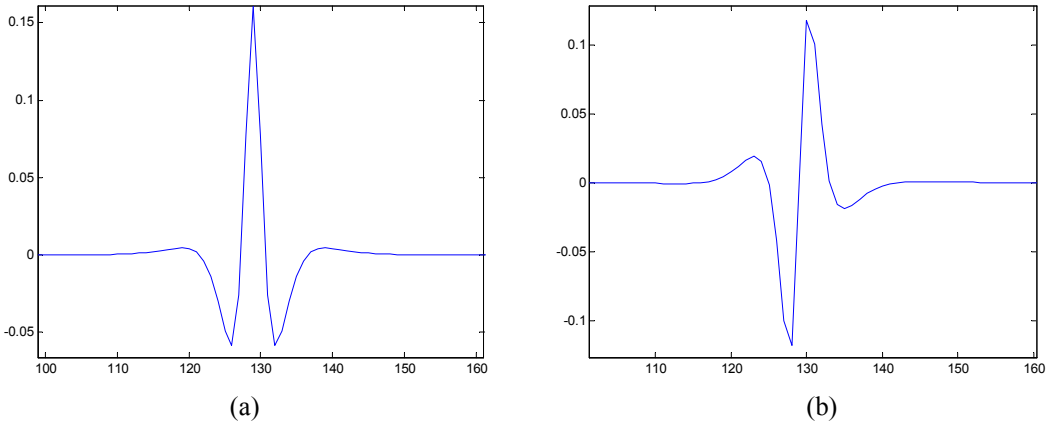


Figure 3: (a) Real and (b) Imaginary Log-Gabor filters in spatial domain having bandwidth of 2 octaves and a center frequency of $1/18$.

The Log-Gabor function has singularity in the log function at the origin, therefore the analytic expression for the shape of the Log-Gabor filter cannot be constructed in spatial domain. Therefore the filter is implemented in frequency domain. The frequency response of Log-Gabor filter in frequency domain is defined as follows:

$$G(f) = \exp\left(\frac{-(\log(f / f_0))^2}{2(\log(\sigma_f / f_0))^2}\right) \quad (4)$$

with f_0 is the central frequency and σ_f is the scaling factor of the radial bandwidth B .

The radial bandwidth in octaves is expressed as follows:

$$B = 2\sqrt{2 / \ln 2} * |\ln(\sigma_f / f_0)| \quad (5)$$

The parameters for the Log-Gabor filter were empirically selected to achieve the

best performance. The decidability index (DI) represents *average* separation of genuine and imposter matching scores and is same as detailed in [22]. However, the optimization of the performance indices obtained from ROC for the most likely operating point of the system (*e.g.* GAR at 0% FAR) is highly desirable and therefore employed to select the parameters of Log-Gabor filter. The center wavelength of 18 and the ratio σ_f / f_0 (sigmaOnf) of 0.55 achieves the best performance as shown in figure 4 and was therefore employed for CASIA I database. Similarly the center wavelength of 22 and σ_f / f_0 equal to 0.55 can achieve best performance as shown in

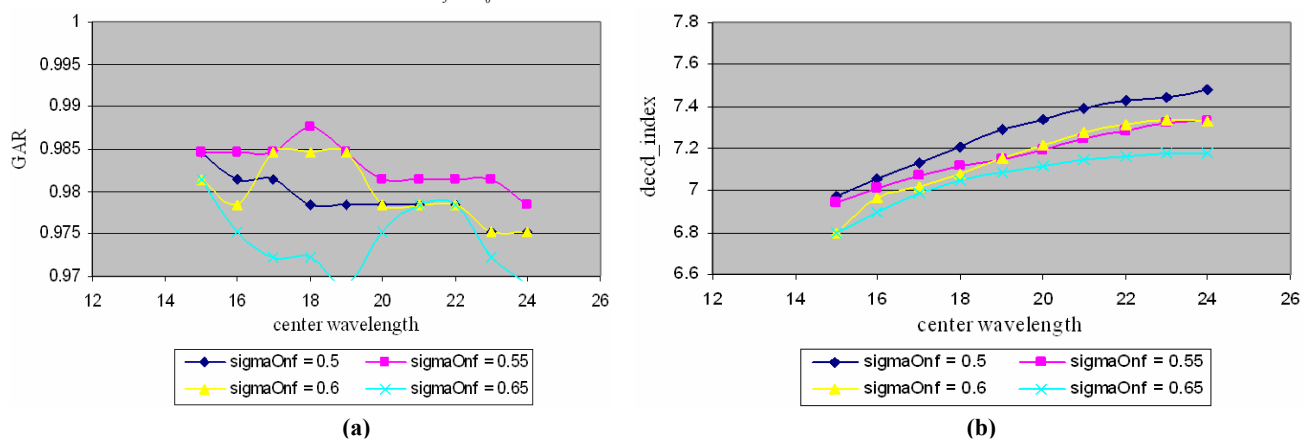


Figure 4: (a) Variation of GAR at 0% FAR and (b) the decidability index as a function of center frequency and bandwidth of Log-Gabor filter for the CASIA I database

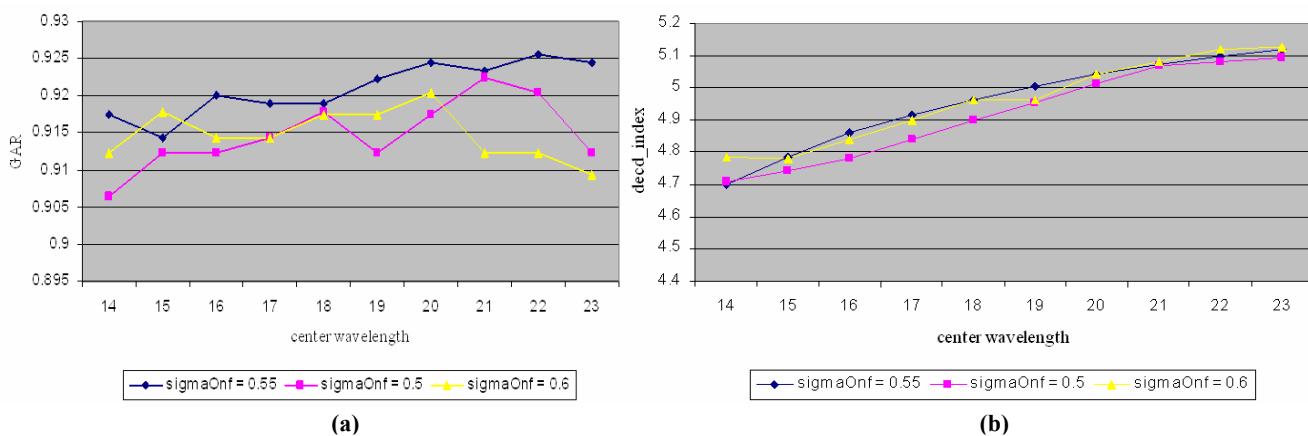


Figure 5: (a) Variation of GAR at 0.01% FAR and (b) the decidability index as a function of center frequency and bandwidth of Log-Gabor filter for the CASIA III database (only first 300 users)

figure 5 for CASIA III database and was therefore selected for the entire performance evaluation reported in this paper.

3. Preprocessing and Normalization

The entire steps for the extraction of normalized iris regions from acquired images were iteratively refined and were efficiently implemented for the online identification.

The pupil in the acquired image usually contains reflection from the illumination source, which forms some bright spots in the pupil, so if the pixel value inside the pupil is over a particular threshold (200) then it is replaced by pixel value of some neighborhood pixel. This operation almost fills the circles but this still it is not good enough to apply a global threshold for the pupil circle estimation. Therefore, as shown

in figure 6, resulting images are further subjected to a 7×7 median filter.

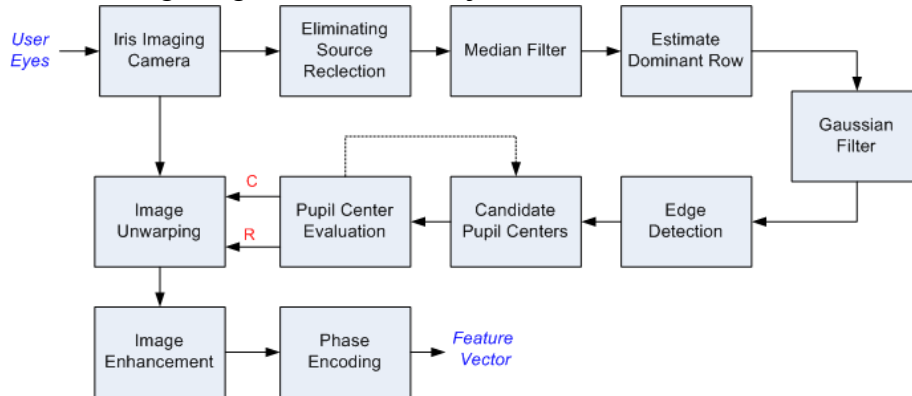


Figure 6: The image normalization steps in our implementation for iris extraction.

The pupil in the resulting images usually appears as a highly distinct black circle. The pupil center in our approach is estimated by scanning the image row-wise and the number of consecutive pixels, whose value is less than certain threshold (say 65 in our implementation), are counted for every row. The row containing the highest number

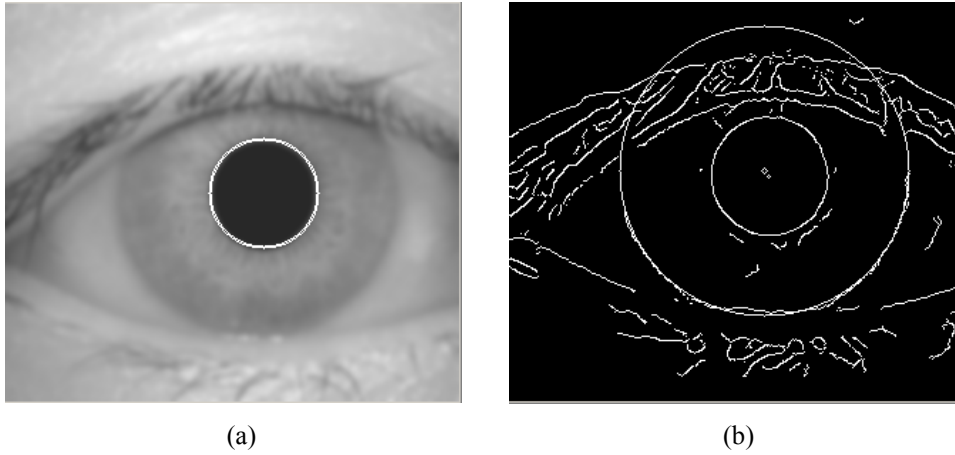


Figure 7: (a) Estimated pupil from the dominant row and (b) the estimated iris boundary from the candidates centers.

of such consecutive pixels must correspond to the diameter of the pupil, half of that maximum value corresponds to the radius of the pupil, the y coordinate of the center of pupil is the row of the diameter and the x coordinate is calculated by adding radius of pupil to the column from where the consecutive pixels started (figure 7). The contrast from the image filtered from the median filter is higher and therefore it's subjected to the Gaussian filtering to remove further noise due to iris texture, then the edge detection is performed using the canny edge detector.

After the edge detection a 20×20 window is chosen in the edge detected image around the center of the pupil. Then every pixel in this window is assumed as the center (candidate centers) and the numbers of white pixels, that are encountered at the perimeter of circle, with radius varying from 80 to 120 pixels, are computed. The winner, *i.e.*, the radius (among 80-120 pixel) and the center (among all 20×20 pixels) for which the maximum white pixels are encountered, is located. That radius R corresponds to the radius of the iris and pixel which was chosen as the center P ,

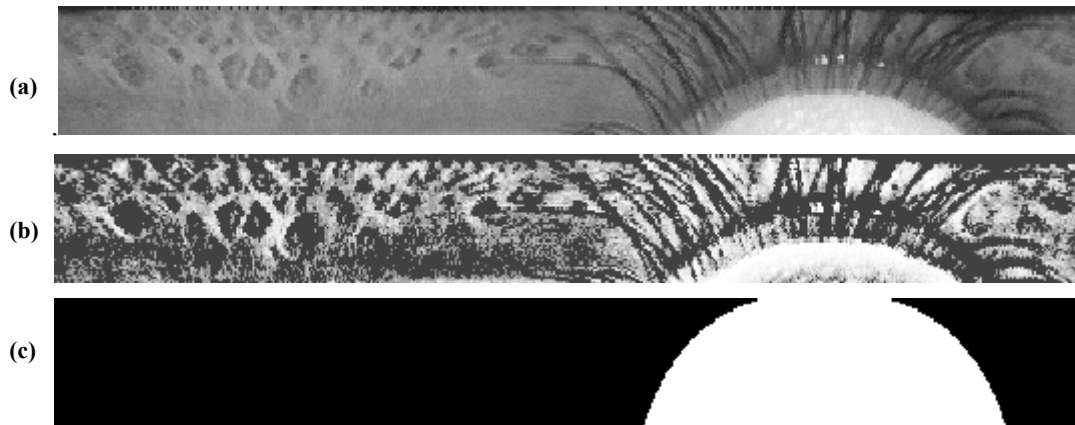


Figure 8: (a) Unwrapped image, (b) enhanced image, and (c) extracted mask

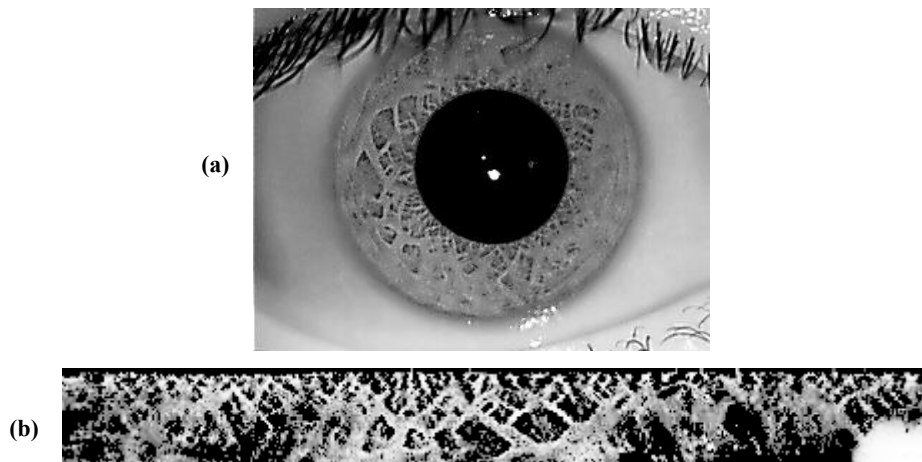


Figure 9: (a) Acquired 320×240 pixel image from the JIRIS JPC1000 Iris camera in IITD database and (b) the corresponding 432×48 pixels unwrapped enhanced image.

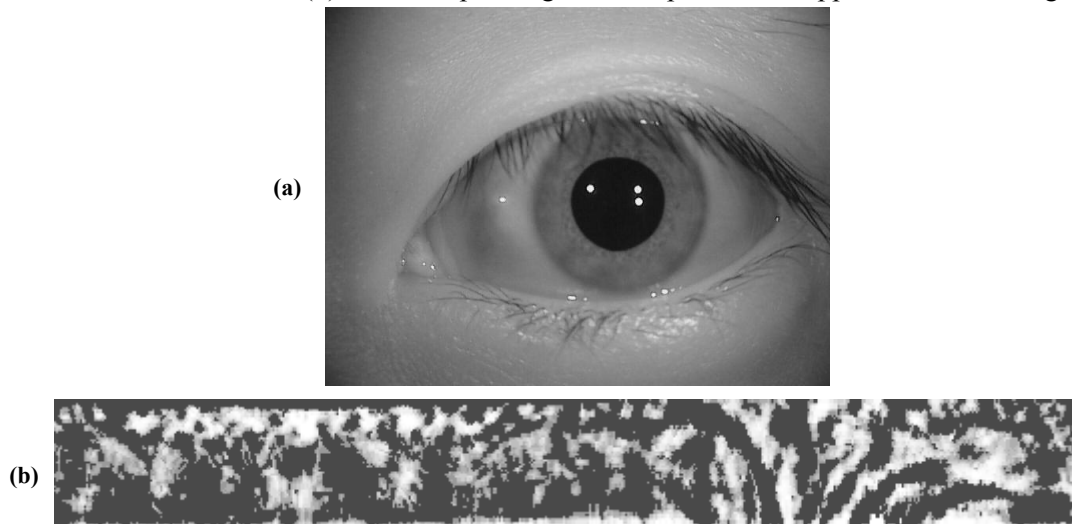


Figure 10: (a) The 640×480 pixel image from CASIA III database and (b) the corresponding 512×64 pixel unwrapped enhanced image

which gave that maximum count, is the center of the iris. Although, this method is computationally more expensive than the methods employed in the literature, but, it

has been experimentally shown to be far more robust. Therefore this method was employed for all the experimental results (from the CASIA I, CASIA III, and IITD database) reported in this paper. The response from the involuntary physiological mechanism, to the varying image acquisition conditions, influences the size of the iris images employed for the feature extraction. In our implementation, the stretching of iris texture due to changes in pupil size is compensated by employing the unwrapping model of iris that can remove the non-concentricity of iris and pupil. The figure 9 shows the unwrapped (also enhanced) rectangular regions of 48×432 pixels from our acquired image sample in IITD database and figure 10 shows the corresponding image sample and its unwrapped region of 64×512 pixels from CASIA III database.

3.1 Combination Strategies

The performance improvement in the unimodal biometrics system can be achieved from the combination of multiple samples, multiple sensors and multiple matchers. The acquisition of multiple iris image samples or the acquisition from multiple sensors highly increases user inconvenience and is therefore not attractive. However, the combination of multiple iris matchers is most promising for online user identification and is therefore investigated in this work. This combination can be typically achieved from the feature-level, matching score-level or the decision-level fusion individual matchers. The phase encoding process employed for the feature

extraction, in all the four matchers considered in section 2, generates binary templates containing bits of information. Therefore feature-level concatenation of these bit-wise templates cannot exploit temporal information contained in the templates from individual matchers. On the other hand, the matching score-level combination usually achieves better performance than decision-level combination. This is due to the fact that score-level representation has higher information content than the abstract class or decisions. The score-level combination offers best trade-off in terms of information content and ease in fusion [32]. Therefore performance improvement using score-level combination of multiple iris matchers is highly promising and investigated in this work.

The combination of matching scores using density-based fusion can offer high accuracy but most complex to implement [31]. In this work, the score-level combination of different iris matchers using fixed fusion rules is employed as they are computationally simple. The combined matching score for every user i , $\forall i = 1, 2, \dots, C$, using Sum, Product and Min rule is obtained as follows:

$$m_a(i) = \frac{1}{Z} \sum_{j=1}^Z s_{ij} \quad (6)$$

$$m_p(i) = \left(\prod_{j=1}^Z s_{ij} \right)^{\frac{1}{Z}} \quad (7)$$

$$m_n(i) = \min_{\forall j} (s_{ij}) \quad (8)$$

where s_{ij} is the individual matching score from i^{th} user using j^{th} matcher, $m_a(i)$, $m_p(i)$, and $m_n(i)$ represents the consolidated matching scores using Sum, Product and Min rule respectively. The Min rule is expected to perform better while consolidating

matching scores having ‘outlier’ type errors. The reference [17] suggests the usage of Product rule for the highly independent matchers and Sum rule for the correlated matchers in which case the errors from the individual matchers are independent. In addition to these rules, one can also generate the consolidated matching score $m_w(i)$ from the weighted combination of individual matching scores;

$$m_w(i) = \sum_{j=1}^Z w_j s_{ij} \quad (9)$$

where $\sum w_j = 1$ and $w_j \geq 0$. The weights w_j indicate the importance of individual matchers and are estimated during training stage using exhaustive search. The computational complexity of combining matching scores, for online user identification, using above considered fixed combination rules is $O(Z*C)$.

4. Experiments and Results

The rigorous experiments were performed to select the parameters that can achieve best possible results. We build-up a new *IIT Delhi Iris Database* from the developed online system which mainly consists of the iris images collected from the students and staff at IIT Delhi, India. This database has been acquired in Biometrics Research Laboratory during Jan - July 2007 using JIRIS, JPC1000, digital CMOS camera [19]. The acquired images were saved in bitmap format. The database of 1120 images is acquired from 224 different users and made available freely to the researchers [16]. All the subjects in the database are in the age group 14-55 years comprising of 176 males and 48 females. The resolution of these images is 320×240 pixels and all these

images were acquired in the indoor environment.

We firstly report the experimental results from the four matchers employed to ascertain the performance from the CASIA I and CASIA III database which is followed by results from the IITD database. The performance from the four considered matchers significantly varies with the increase in number of training images. Therefore the experiments were performed to ascertain the performance improvement with varying number of training images.

The figure 11(a) illustrates the ROC from the DCT based approach detailed in section 2.1. Similarly, figure 11(b) illustrates the ROC from the FFT based approach as detailed in section 2.2. Significant increase in the performance can be observed with the increase in number of training images while the DCT based approach achieves much better performance as compared to the approach using FFT features.

The figure 12 illustrates individual performance from the Haar wavelet and Log-Gabor filter approach.

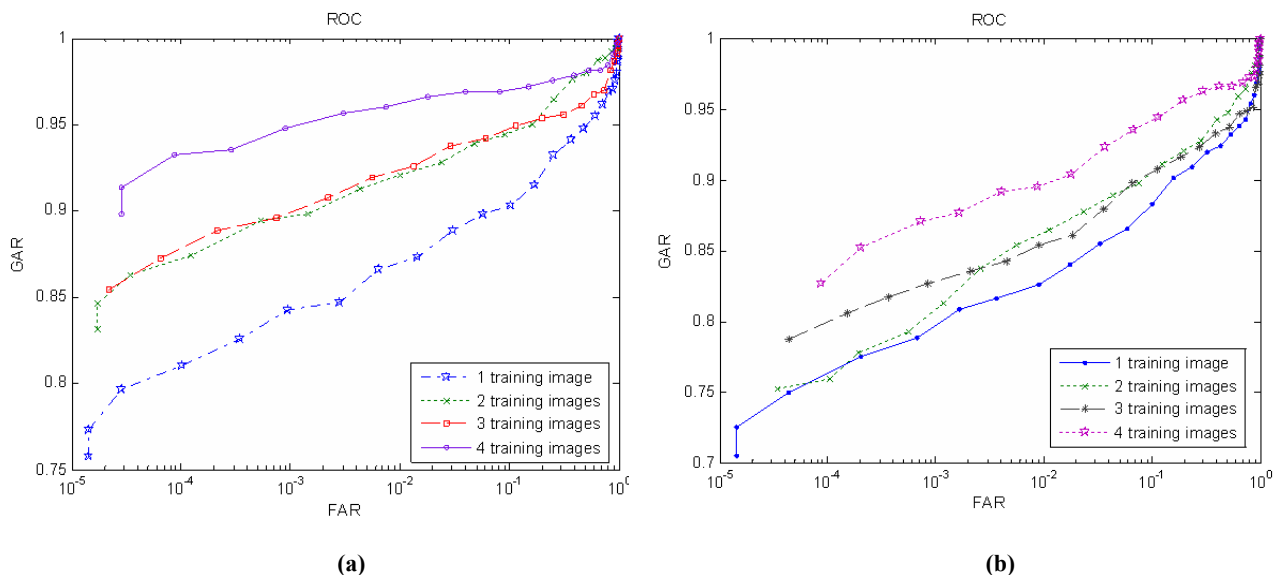


Figure 11: The ROC from the test data using (a) DCT based and (b) FFT based approach.

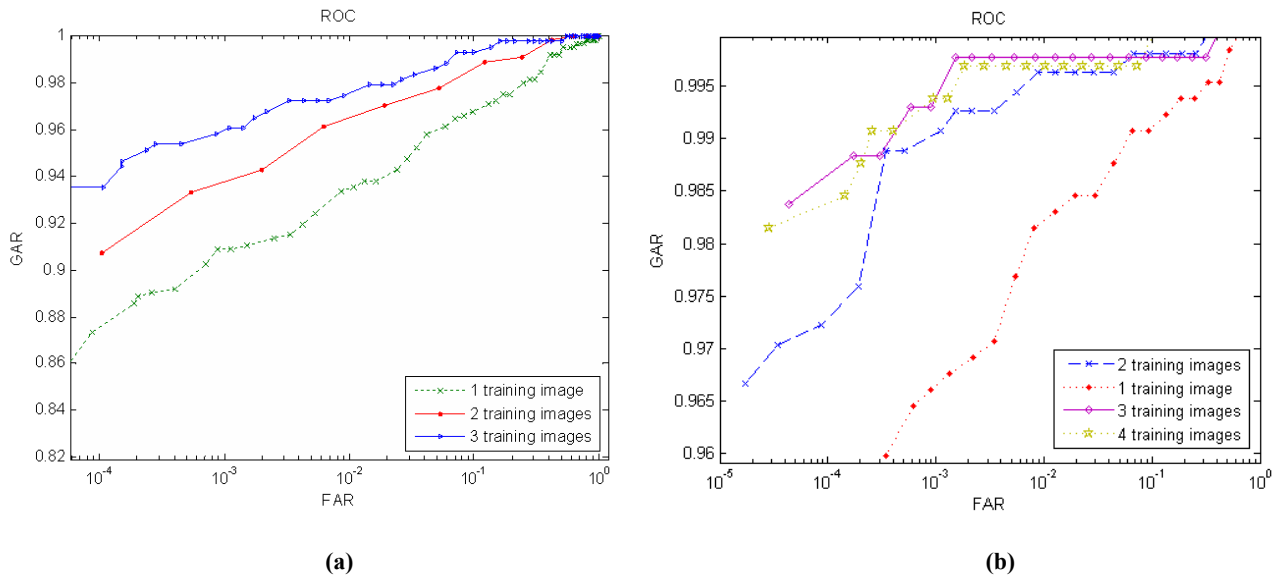


Figure 12: The ROC from the test data using (a) Haar wavelet, and (b) log- Gabor filter based approach.

The performance from the Log-Gabor filter shown in figure 12(b) is observed to be the best among all the four considered approaches, however its performance does not improve as the number of training images are increased from three to four. This is possibly due to the overtraining from the increase in number of training images. The performance from the FFT based approach (figure 11-b) has been the worst among the four considered approaches and therefore this approach was not considered for the score level fusion.

We performed rigorous experiments for the score level combination of best performing three approaches using fixed combination rules. The experimental results from the score level combination using only one/first training image are illustrated in figure 13 and 14. The figure 13 suggests that the performance from the product and min rule has not been effective in improving the performance. However, the weighted

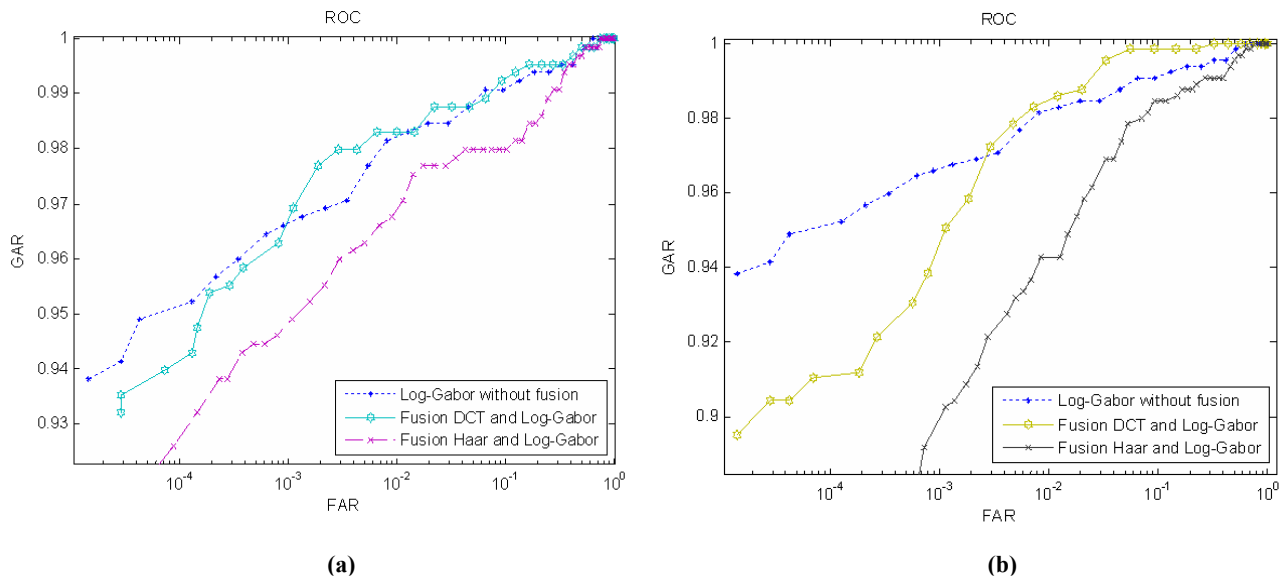


Figure 13: The fusion of Haar and DCT with Log-Gabor scores using Product rule in (a), and Min rule in (b).

sum rule is quite effective in achieving the performance improvement as can be observed from results in figure 14. It can be observed from this figure that the performance improvement from the Haar wavelet and the Log-Gabor filter is significantly higher than those from the DCT and the Log-Gabor filter. Figure 14 (b) summarizes the performance from the combination of DCT scores with those from Log-Gabor using various fixed rules and suggest that even the best results from weighted sum rule does not achieve any appreciable improvement in the performance.

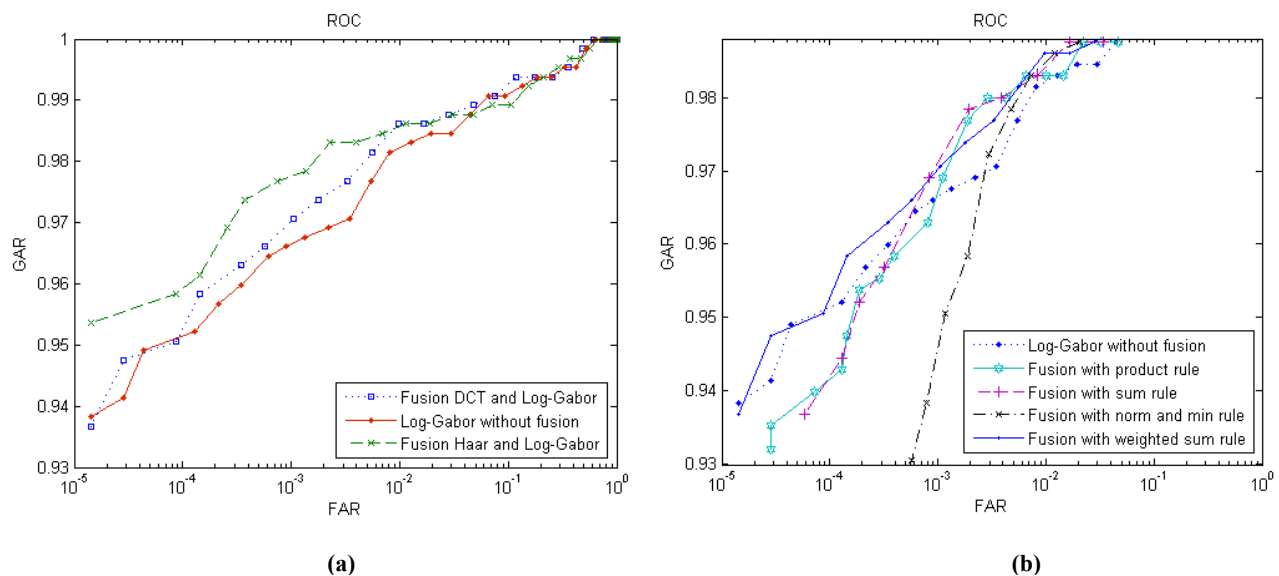


Figure 14: The ROC using weighted sum rule combination from DCT, Haar and Log-Gabor scores in (a), and comparison of performance from DCT and Log-Gabor using different combination rules in (b).

Furthermore, the Haar wavelet approach requires least amount of computations among all approaches and can be implemented with simple integer processing. Therefore this combination is the most promising to achieve the performance improvement and was further investigated. The equal error rate (EER shown in %) and the decidability index (DI) were used to as the quantitative performance indices to ascertain the performance [22]. Table 1 presents the summary of these performance indices on the CASIA I database. The performance indices in this table suggests significant improvement in the performance while simultaneously combining the scores from the Log Gabor and Haar wavelet based matching.

Table 1: Performance Indices from the experiments using CASIA I database.

	One Training		Two Training	
	<i>EER</i>	<i>DI</i>	<i>EER</i>	<i>DI</i>
Log-Gabor Filter	1.62	5.4808	0.55	6.4463
Haar Wavelet	4.43	4.6679	2.96	5.3318
Fusion	0.94	5.6948	0.36	6.7175

The proposed approach to achieve the performance improvement was also investigated on CASIA III (lamp) iris image database [14]. We employed 2877 left eye images from all the 411 users to ascertain the performance. Our experiments employed first seven images from all 411 users simply to limit the large computations involved in generating imposter scores. The experimental results from the CASIA III database are summarized in table 2 and also shown in figure 15. Each of the ROC's shown in figure 14 employed 1,011,060 ($411 \times 410 \times 6$) imposter matching scores and

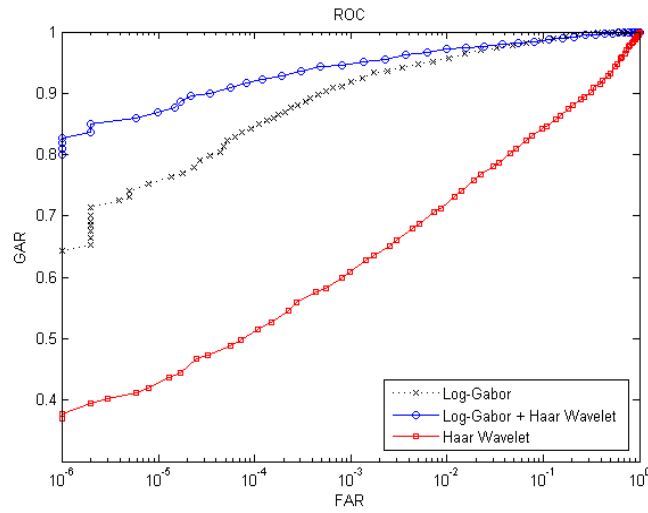


Figure 15: The performance from CASIA III database using one training image

Table 2: Performance Indices from the experiments using CASIA III database.

	<i>EER</i>	<i>DI</i>
Log Gabor Filter	3.72	4.7543
Haar Wavelet	13.16	2.8078
Fusion	2.40	4.6993

2466 (411×6) genuine matching scores. It can be ascertained from ROC in figure 15 that the performance improvement, due to the simultaneous usage of Haar wavelet features, is significant. In addition, the IIT Delhi iris database [16] was also used to ascertain the performance improvement. The methods for the performance evaluation

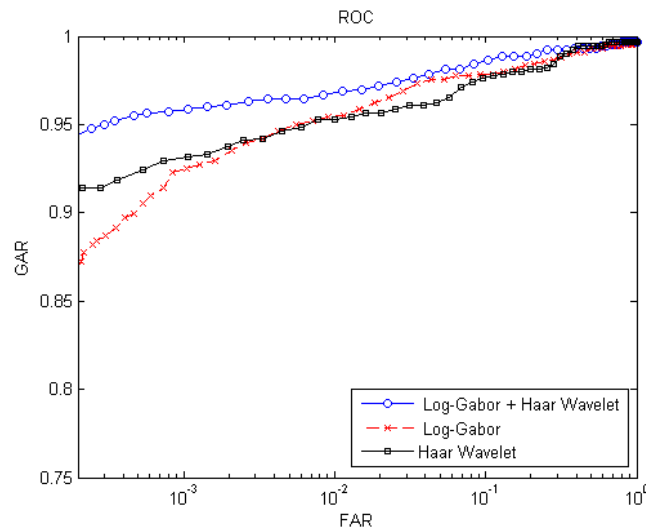


Figure 16: The performance from IITD database using first/one training image.

on IIT Delhi database were same as used for the CASIA I database. The performance from the IITD database using the one/first training image is presented in figure 16. The results illustrate the performance improvement due to the simultaneous usage of Log-Gabor and Haar wavelet features. In order to ascertain the performance improvement from minimum training image, independent of the training image, rigorous experiments were performed to ascertain the average performance. In these set of experiments average of results obtained when each of the eight (five for IITD database) images were employed for training and rest of the images as the test set. The average performance from the IITD database and CASIA I database is summarized in the table 3. The corresponding ROCs are illustrated in figure 17. The performance indices shown in table 3, from this set of experiments, suggest that the achieved performance improvement is quite independent of selected training image.

The proposed system is implemented in Visual C++ 6.0 on Windows operating system

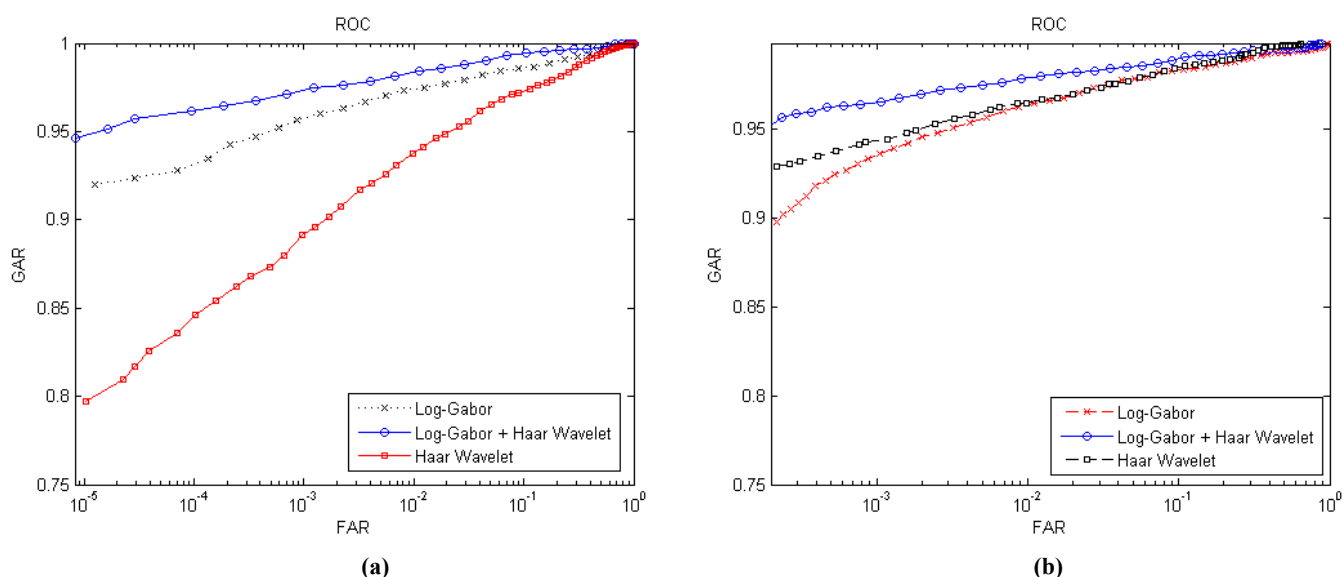


Figure 17: The average performance from (a) CASIA I and (b) IITD database using one training image.

Table 3: Performance Indices from the average experiments IITD and CASIA I database.

	IITD		CASIA I	
	<i>EER</i>	<i>DI</i>	<i>EER</i>	<i>DI</i>
Log Gabor Filter	2.81	5.7437	2.21	5.2884
Haar Wavelet	3.40	6.1762	3.91	4.8016
Fusion	2.59	6.4079	1.48	5.6640

environment.

5. Discussion

One of the key challenges in the comparison of performance from the various feature extraction algorithms relates to the selection of the parameters. Therefore we iteratively selected the different set of parameters, as detailed in section 2, to achieve the best performance corresponding to the employed database. The CASIA I database is by far the most widely used iris database for the performance evaluation in the literature [7] and has often been cited as standard benchmark for iris algorithms [1]. The recent comments [18] on CASIA I database suggests that images in this dataset have their pupil regions masked to suppress the specular reflections from the near IR illuminators. However, such reflections have been conveniently removed in the pre-processing stage by the inclusion of a median filter as shown in figure 6. These reflections are common in CASIA III and IIT Delhi database and thus our implementation does not have any problem in handling pupils with such specular reflections (sample results in figure 9 and 10). Therefore we also investigated the performance on CASIA I database, as this database has been extensively used in

several of prior publications, and achieved similar or better performance improvement. The experimental results from the CASIA I database using Gabor filters have also been presented in [5] [33]. The experimental results in [5] achieve EER of 0.09% while in [33] the author's have not provided any estimate of EER. However, it is very difficult to compare our results with this work since only a portion of CASIA I database is *publicly* made available and all of which has been employed in our work (while [5] [33] utilize full version of this database). The experimental results shown in table 1-3 should be seen in the context of single training image and achieved performance can be significantly improved with the increase in number of training images (table 1).

Our experimental results in section 4 from the comparison of the four approaches illustrated that the Log-Gabor and Haar wavelet achieves the best performance among the four considered approaches. The performance from Log-Gabor features was best on CASIA I and CASIA III database. However, the achieved performance (figure 16 and 17) on IITD database was superior from the Haar wavelet features as compared to those from Log-Gabor features. These observations suggest that the performance from the feature extraction algorithms also depend on the employed database (nature of images). Despite the variations in the absolute performance among three databases, the significant performance improvement is consistently observed while combining

the scores from the two approaches. The experimental results presented from the CASIA III database, from all 411 users, involved over 12 million ($12 \times 1,011,060$) comparisons. In our work, we employed first seven images from each of the 411 users, to limit the complexity involved in significantly large number of matching. However, to the best of our knowledge, these results involve the largest number of matching operations yet presented from any *publicly* available iris database.

The observed performance from the IITD database (figure 16 and 17) is generally poor, as compared to those from CASIA I and CASIA III database. This could be possibly due to the fact that IITD database contains low-resolution and also poor quality images, as compared to CASIA database. This database employed a low-cost iris camera (370 US\$) for imaging and the presence of poor quality iris images can significantly degrade the performance [23].



Figure 18: Some low quality image samples from IITD iris database.

6. Conclusions

This paper has investigated the comparative performance from four different approaches for the iris identification: DCT, FFT, Haar wavelet and Log-Gabor filter.

Our experimental results presented in previous section suggest that the performance from the performance from the Log-Gabor filter is the best which is followed by the Haar wavelet, DCT and FFT in order. This paper has also investigated the possible performance improvement using score-level combination. The experimental results suggest that the combination of Log-Gabor and Haar wavelet matching scores using weighted sum rule is the most promising. The Haar wavelet based approach is also the most attractive as it requires minimum computational time and can be easily implemented in fixed point environment. The extensive evaluation of the proposed combination on CASIA I (108 users), CASIA III (411 users) and IITD (224 users) database achieved significant improvement in the performance. The summary of prior work presented in section 1.2 has suggested that prior efforts have been employing several training images for the performance evaluation. However, the performance evaluation presented in this paper has been focused on usage of one training image.

The motivation for considering only fixed combination rules in this paper was the fact that this approach does not require any training and is computationally simpler. However, the trainable fusion strategies may offer better performance improvement and is suggested for the investigation in the future efforts. The pupil detection algorithm developed in this works well for the three public databases used for performance evaluation and assumes that user eyes does not have large specular

reflections from the surface of glass that might be present. The presence of large specular reflection and thick black glass frame will limit the accuracy of the performance from the employed iris segmentation approach. Therefore further efforts are required to develop more accurate iris segmentation method that can be robust to handle such large specular reflection in presence of glasses. Also, this work has been focused on the user authentication and an extension of this work should evaluate the performance for recognition. Even though the speed of developed online system is fast (authenticates individuals in less than a second), we are working to further optimize by using better coding techniques (multithreaded implementation).

7. Acknowledgement

We thankfully acknowledge the Chinese Academy of Sciences Institute of Automation for providing us the CASIA I and CASIA III Iris Image Database.

8. References

- [1] J. Thornton, M. Savvides, B. V. K. Vijay Kumar, "A Bayesian approach to deformed pattern matching of iris images," *IEEE Trans. Patt. Anal. Machine Intell.*, vol. 29, pp. 596-606, Apr. 2007.
- [2] J. Daugman, "High confidence visual recognition of persons by a test of statistical independence," *IEEE Trans. Patt. Anal. Machine Intell.*, vol. 15, pp. 1148-1161, Nov. 1993.
- [3] D. M. Monro, S. Rakshit, and D. Zhang, "DCT-based iris recognition," *IEEE Trans. Patt. Anal. Machine Intell.*, vol. 29, pp. 586-595, Apr. 2007.
- [4] W. W. Boles, "A security system based on human iris identification using wavelet transform," *Proc. Intl. Conf. Knowledge-Based Intelligent Electronic Systems*, pp. 533-541, May 1997.
- [5] L. Ma, T. Tan, Y. Wang, and D. Zhang, "Efficient iris recognition by characterizing key local variations," *IEEE Trans. Image Process.*, vol. 13, pp. 739-750, 2004.
- [6] R. P. Wildes, "Iris recognition: An emerging biometric technology," *Proc. IEEE*, vol. 89,

- no. 9, pp. 1348-1363, Sep. 1997.
- [7] H. Proença and L. A. Alexandre, "Towards noncooperative iris recognition: A classification approach using multiple signatures," *IEEE Trans. Patt. Anal. Machine Intell.*, vol. 29, pp. 607-612, Apr. 2007.
- [8] L. Flom and A. Safir, "Iris Recognition System," *US Patent No. 4 641 394*, 1987.
- [9] E. Stollnitz, T. DeRose, and D. Salesin, *Wavelet for Computer Graphics: Theory and Applications*, Morgan Kaufmann, 1996.
- [10] L. Shinyoung, K. Lee, O. Byeon. "Efficient Iris Recognition Through Improvement Of Feature Vector And Classifier", *ETRI Journal*. vol. 23, pp. 61-70, June 2001.
- [11] C. H. Daouk, L.A. Esber, F. O. Kanmoun, and M. A. Alaoui, "Iris Recognition", *Proc. ISSPIT*, pp. 558-562, 2002.
- [12] L. Masek, *Recognition of human iris pattern for biometric identification*, B. Eng. Thesis, University of Western Australia, 2003.
<http://www.csse.uwa.edu.au/~pk/studentprojects/libor/index.html>, 2008
- [13] P. Yao, J. Li, X. Ye, Z. Zhuang and B. Li, "Iris Recognition using modified Log-Gabor filters," *Proc. ICPR 2006*, Hong Kong, pp. 1-4, Aug. 2006.
- [14] D. Fields, "Relations between the statistics of natural image and the response properties of cortical cells," *J. Optical Soc. America*, vol. 4, no. 12, pp. 2379-2394, 1987.
- [15] CASIA IRIS Database, <http://www.cbsr.ia.ac.cn/english/IrisDatabase.asp>, 2008
- [16] IITD Iris Database, http://web.iitd.ac.in/~biometrics/Database_Iris.htm, 2008
- [17] D. M. J. Tax, M. V. Breukelen, R. P. W. Duin and J. Kittler, "Combining multiple classifiers by averaging or combining," *Pattern Recognition*, vol. 33, pp. 1475-1485, 2000.
- [18] P. J. Phillips, K. W. Bowyer and P. J. Flynn, "Comments on the CASIA version 1.0 iris dataset," *IEEE Trans. Patt. Anal. Machine Intell.*, vol. 29, pp. 1869-1870, Oct. 2007.
- [19] <http://www.jiristech.com/english/products/iris.php>, 2008
- [20] J. Huang, T. Tan, L. Ma, Y. Wang, "Phase correlation based iris image registration model," *Computer Science and Technology*, vol. 20, no. 3, pp. 419-425, May 2005.
- [21] J. Daugman, "Probing the uniqueness and randomness of IrisCodes: Results from 200 billion iris pair comparisons," *Proc. IEEE*, vol. 94, no. 11, pp 1927-1935, 2006.
- [22] J. Daugman, "How Iris recognition works," *IEEE Trans. Circuits & Sys. Video Tech.*, vol. 14, pp. 21-30, Jan. 2004.
- [23] Y. Chen, S. Dass, and A. K. Jain, "Localized iris image quality using 2-D wavelets," *Proc. ICB*, Hong Kong, pp. 373-381, Jan. 2006.
- [24] L. Ma, T. Tan, Y. Wang and D. Zhang, "Local intensity variation analysis for iris recognition," *Pattern Recognition*, vol. 37, no. 6, pp. 1287-1298, Jun. 2004.
- [25] M. Nabti and A. Bouridane, "An effective and fast iris recognition system based on a combined multiscale feature extraction technique," *Pattern Recognition*, vol. 41, no. 3,

pp. 868-879, Mar. 2008.

- [26] X. He and P. Shi, "A new segmentation approach for iris recognition based on hand-held capture device," *Pattern Recognition*, vol. 40, no. 4, pp. 1326-1333, Apr. 2007.
- [27] W. K. Kong and D. Zhang, "Detecting eyelash and reflection for accurate iris segmentation," *Int. J. Pattern Recognition*, vo. 17, no. 6, pp. 1025-1034, 2003.
- [28] L. Yu, D. Zhang and K. Wang, "The relative distance of key point based iris recognition," *Pattern Recognition*, vol. 40, no. 2, pp. 323-430, Feb. 2007.
- [29] L. Yu, D. Zhang, K. Wang and W. Yang, "Coarse iris classification using box-counting to estimate fractal dimensions," *Pattern Recognition*, vol. 38, no. 11, pp. 1791-1798, Nov. 2005.
- [30] C. Sanchez-Avila and R. Sanchez-Reillo, "Two different approaches for iris recognition using Gabor filters and multiscale zero-crossing representation," *Pattern Recognition*, vol. 38, no. 2, pp. 231-240, Feb. 2005.
- [31] B. Ulery, A. R. Hicklin, C. Watson, W. Fellner, and P. Hallinan, "Studies of Biometric Fusion," *NIST Technical Report No. IR 7346*, Sep. 2006.
- [32] K. Nandakumar, Y. Chen, S. C. Dass and A. K. Jain, "Likelihood Ratio Based Biometric Score Fusion," *IEEE Trans. Patt. Anal. Machine Intell.*, vol. 30, pp. 342-347, Feb. 2008.
- [33] L. Ma, T. Tan, Y. Wang, and D. Zhang, "Personal identification based on iris texture analysis," *IEEE Trans. Patt. Anal. Machine Intell.*, vol. 25, pp. 1519-1533, 2003.